hep-ph/0308068

SHEP-03/26

Implications of $B_s \to \mu^+\mu^-$ in $SO(10)$-like Models

T. Blažek*, S. F. King and J. K. Parry

Department of Physics and Astronomy, University of Southampton

Southampton, SO17 1BJ, U.K

Abstract

We examine the potentially very promising signal $B_s \to \mu^+\mu^-$ in supersymmetry with large $\tan\beta$ in a *top-down* approach starting from the best fits of an $SO(10)$-like model studied recently. Our results go beyond minimal flavour violation investigated in previous works. We show that the absolute best fits provide a signal for $B_s \to \mu^+\mu^-$ at the borderline of the present limits and hence the ongoing search at the Tevatron will start having an impact on the global analysis of this class of SUSY models. We discuss the implications of a measurement of $B_s \to \mu^+\mu^-$ for restricting the parameter space of gauginos and sfermion masses, and of signals in other channels $B_{d,s} \to \ell^+\ell^-$. We also discuss correlations of $B_s \to \mu^+\mu^-$ with the CP-odd Higgs mass, $\sin(\beta-\alpha)$ and $b \to s\gamma$ in $SO(10)$-like models.

February 7, 2008

*On leave of absence from the Dept. of Theoretical Physics, Comenius Univ., Bratislava, Slovakia

1 Introduction

Ideas of unification and the origin of flavour have been under investigation for a long time and many different models have been proposed in the last twenty years. Yet in the diversity of different approaches a class of unification models can be recognised which is remarkably simple at the unification scale. We call this class SO(10)-like unification models. In these models the effective theory at the unification scale assumes that the Standard Model (SM) gauge couplings unify to a per cent level, third family yukawa couplings are all of order unity and the remaining flavour structure originates in a small set of higher-dimensional superpotential operators keeping the supersymmetry (SUSY) breaking sector of a model flavour blind. We note that actual models which fall into this category often assume lower symmetry than SO(10), e.g. models based on the Pati-Salam gauge group or the MSSM gauge group generated by a string theory in higher dimensions are often found in this class of models.

It has been recently pointed out that if the Minimal Supersymmetric Standard Model (MSSM) is the effective theory describing nature above the scale 100 GeV and $\tan\beta \equiv \langle H_u^0 \rangle \,/\, \langle H_d^0 \rangle \equiv v_u/v_d$ is large, a pure leptonic $B_s \to \mu^+\mu^-$ decay has a very strong case to emerge among the first indirect signals of supersymmetry (SUSY) [1]. This is because the decay signal should be very clear at the Tevatron or LHC and also because the SM branching fraction is suppressed down to 10^{-9} while the rate can be enhanced when considering SUSY extensions. In particular, this occurs due to large couplings of the down-type quarks and charged leptons to the MSSM higgs states if $\tan\beta$ is large. Thus it is important to analyse this decay in a full SUSY theory and not just in terms of the minimal flavour violation that assumes that V_{cb} is the only source of the 32 transition, as has been done in the past. In the full context of complete unification models it means that the 32 flavour structure is restricted by the fermion mass ratios m_μ/m_τ, m_s/m_b and m_c/m_t, small value of V_{cb}, large $U_{\mu 3}$,

$b \to s\gamma$ branching ratio and possibly other low energy observables and constraints. Although these constraints do not determine the 32 sector uniquely they do provide for a realistic prediction of observables like the $B_s \to \ell^+\ell^-$ decay rates.

In this letter we present the results of such a complete *top-down* investigation based on the best fit predictions obtained in a recent global analysis of a complete SO(10)-like model [2]. The best fits obtained in this work give a very good agreement with the observables related to 32 flavour sector and satisfy all laboratory experimental constraints on superpartner masses. Here they serve as our starting point since they provide us with all the MSSM couplings at the low-energy scale. Within this framework we study the implications of a possible measurement $B_s \to \mu^+\mu^-$. In particular, we discuss the related processes $B_s \to \tau^+\tau^-$, $B_d \to \mu^+\mu^-$, $B_d \to \tau^+\tau^-$, and show the correlations with $B_s \to \mu^+\mu^-$. We discuss the implications of a measurement of $B_s \to \mu^+\mu^-$ for restricting the parameter space of gauginos and sfermion masses, and also discuss correlations of $B_s \to \mu^+\mu^-$ with $b \to s\gamma$ and the CP-odd Higgs mass.

After this introduction the letter continues in section 2 with a brief theoretical section on the evaluation of $B_s \to \ell^+\ell^-$ decay rate in *top-down* approach. In section 3 we give some brief discussion of the $SO(10)$-like model we study. Section 4 contains our numerical results, and a discussion of the implications of a signal for $B_s \to \mu^+\mu^-$ mentioned above. Section 5 concludes the paper.

2 $B_s \to \mu^+\mu^-$

We emphasise that in a *top-down* approach the tree-level MSSM couplings are determined from high energy boundary conditions, and do not have to be determined by an iterative proceedure as in bottom-up approaches. In particular, in terms of effective vertices f and g, which are matrices in flavour space, after heavy sparticles

are integrated out the lagrangian can be written down as

$$\mathcal{L}_{eff} = -\overline{d}_R^{(0)} \left[Y_d^{(0)\mathrm{Diag}\,\dagger} H_d^0 + f^\dagger H_d^0 + g^\dagger H_u^{0\,*} \right] d_L^{(0)} + h.c.. \tag{1}$$

At tree level down-type quarks $d_{L,R}$ only couple to down-type Higgs H_d^0 and $f = g = 0$. Yukawa couplings $Y_d^{(0)}$ can be read out as a straightforward prediction of a unified model. $Y_d^{(0)}$ and the mass matrix $m_d^{(0)} = Y_d^{(0)} v_d$ can then be simultaneously diagonalised with eigenvectors $d_{R,\,L}^{(0)}$. At one-loop level f and g have to be computed and the mass terms relevant for this discussion become [1]

$$\mathcal{L}_{mass} = -\overline{d}_R^{(0)} \left[m_d^{(0)\mathrm{Diag}\,\dagger} + f^\dagger v_d + g^\dagger v_u \right] d_L^{(0)} \tag{2}$$

using the same basis. Clearly, if $v_u \gg v_d$ sizeable corrections to the mass eigenvalues [3] and mixing matrices [4] are generated. Furthermore the 3-point functions in (1) and mass matrix in (2) cannot be simultaneously diagonalised [5]. If we write eq. (1) as

$$-\overline{d}_R^{(0)} \left[Y_d^{(0)\mathrm{Diag}\,\dagger} + f^\dagger + g^\dagger \frac{v_u}{v_d} \right] d_L^{(0)} H_d^0 \; - \; \overline{d}_R^{(0)} \left[g^\dagger \left(H_u^{0*} - \frac{v_u}{v_d} H_d^0 \right) \right] d_L^{(0)} \tag{3}$$

then the first bracket of eq. (3) is in a form which is similar to that of the mass matrix and therefore is diagonal when $d_{L,\,R}^{(0)}$ are rotated into corrected mass eigenstates $d_{L,\,R}^{(1)} = V_d^{L,R\,(1)} d_{L,\,R}^{(0)}$. This is not true for the last bracket which becomes a source of flavour changing,

$$\mathcal{L}_{FCNC} \;=\; -\overline{d}_{R\,i}^{(1)} \left[V_d^{R\,(1)} g^\dagger \left(H_u^{0*} - \frac{v_u}{v_d} H_d^0 \right) V_d^{L\,(1)\,\dagger} \right]_{ij} d_{L\,j}^{(1)} + h.c., \tag{4}$$

It is now explicit that its origin comes from the interaction $\overline{d}_R^0 H_u^{0*} d_L^0$, not present at tree level. Moreover, the flavour changing couplings get enhanced by an explicit factor $\tan\beta$ on top of any $\tan\beta$ scaling present in g. In the leading order in $\tan\beta$ the g matrix can in fact be related in a simple way to the finite non-logarithmic mass matrix corrections, $g_{ij} = (\delta m_d^{finite})_{ij}/v_u$, computed for the first time in [4]. Due to $H_u^0 =$

[1] Terms due to wavefunction renormalisation do not contribute to flavour changing.

$v_u+(H^0 s_\alpha+h^0 c_\alpha+iA^0 c_\beta+iG^0 s_\beta)/\sqrt{2}$ and $H_d^0 = v_d+(H^0 c_\alpha-h^0 s_\alpha+iA^0 s_\beta-iG^0 c_\beta)/\sqrt{2}$ we can write

$$H_u^{0*} - \frac{v_u}{v_d} H_d^0 \;=\; \frac{1}{\sqrt{2}}\,\frac{1}{c_\beta}\left[H^0 s_{\alpha-\beta} + h^0 c_{\alpha-\beta} - i\,A^0\right], \tag{5}$$

where $s_\alpha \equiv \sin\alpha$, $c_\alpha \equiv \cos\alpha$, *etc.* We can thus identify effective vertices $\overline{b}_R s_L H^0$, $\overline{b}_R s_L h^0$ and $\overline{b}_R s_L A^0$ involving b to s transitions mediated by neutral physical higgs states. We note that with large $\tan\beta$ the coupling to the pseudoscalar A^0 is always large while the CP-even states, h^0 and H^0, have couplings which depend on the CP-even higgs mixing angle α. The Goldstone mode is cancelled in the equation above and thus the effective vertex with the Z boson is absent at this level.

In the MSSM with large $\tan\beta$ the dominant contribution to $B_s \to \ell^+\ell^-$ comes from the penguin diagram where the dilepton pair is produced from a virtual Higgs state [1]. After the SUSY partners are integrated out we are left with the effective vertices determined above. Thus in combination with the standard tree-level term $\mathcal{L}_{\ell\ell H} = -y_\ell \overline{\ell_R}\ell_L H_d^0 + h.c.$ the dominant $\tan\beta$ enhanced contribution to the branching ratio turns out to be

$$\begin{aligned} BR(B_s^0 \to \mu^+\mu^-) \;&=\; 2.25\times 10^{-3}\,\left|\frac{\delta m_{d\,32}^\dagger}{m_b V_{ts}}\right|^2\,\left[\frac{V_{ts}}{0.04}\right]^2\left[\frac{y_\mu}{0.0353}\right]^2\left[\frac{M_{170}}{v_u}\right]^2\left[\frac{\tan\beta}{50}\right]^2 \;\times \\ &\times\;\left[\left(\frac{c_\alpha s_{\alpha-\beta}}{\left(\frac{M_{H^0}}{M_{100}}\right)^2} - \frac{s_\alpha c_{\alpha-\beta}}{\left(\frac{M_{h^0}}{M_{100}}\right)^2}\right)^2 + \frac{s_\beta^2}{\left(\frac{M_{A^0}}{M_{100}}\right)^4}\right], \end{aligned} \tag{6}$$

where matrix $\delta m_d^\dagger$ is in the $\{d_{L,R}^{(1)}\}$ basis, and is defined by

$$\delta m_d^\dagger = V_d^{R\,(1)}(f^\dagger v_d + g^\dagger v_u)V_d^{L\,(1)\dagger}, \tag{7}$$

m_b is the b quark mass at scale M_Z in the effective $SU(3)_c \times U(1)_{em}$ theory, the constants are $M_{100} = 100\,\mathrm{GeV}$ and $M_{170} = 170\,\mathrm{GeV}$ and the numerical value is obtained from

$$2.25\times 10^{-3} \;=\; \frac{\tau_B f_B^2 M_B^5}{128\pi}\;\frac{0.04^2\,0.0353^2\,50^2}{M_{100}^4\,M_{170}^2}. \tag{8}$$

Modification for other $B^0_{d_i} \to \ell^+\ell^-$ decays is trivial. We note that each of these branching fractions actually scales down as $\tan^6\beta$ for lower values of $\tan\beta$: additional powers of $\tan\beta$ enter due to the explicit presence of lepton yukawa coupling y_ℓ^2 and mass matrix corrections $\delta m_d^{finite}/m_b$ (or, equivalently, yukawa coupling y_{d_i} in g).

3 An $SO(10)$-like Model

Our results are based on the model analysed in [2]. The model was defined below the $SO(10)$ breaking scale, where the gauge group was broken to its maximal Pati-Salam subgroup, and the flavour structure of the model was determined by operators which respected the Pati-Salam symmetry. Universal gaugino masses $M_{1/2}$ and sfermion masses m_F were assumed, and we allowed for D-terms and non-universal Higgs masses. Throughout this work the trilinear parameter was kept fixed at $A_0 = 0$. More details concerning the model can be found in [2], however the Yukawa matrices which enter at the unification scale are listed below for completeness:

$$Y_u(M_{GUT}) = \begin{pmatrix} \sqrt{2}\,a''_{11}\lambda^8 & \sqrt{2}\,a'_{12}\lambda^5 & \frac{2}{\sqrt{5}}\,a'_{13}\lambda^3 \\ 0 & \frac{8}{5\sqrt{5}}\,a'_{22}\lambda^4 & 0 \\ 0 & \frac{8}{5}\,a'_{32}\lambda^4 & r_t a_{33} \end{pmatrix}$$

$$Y_d(M_{GUT}) = \begin{pmatrix} \frac{8}{5}\,a_{11}\lambda^6 & -\sqrt{2}\,a'_{12}\lambda^5 & \frac{4}{\sqrt{5}}\,a'_{13}\lambda^3 \\ \frac{2}{\sqrt{5}}\,a_{21}\lambda^5 & \sqrt{\frac{2}{5}}\,a_{22}\lambda^3 + \frac{16}{5\sqrt{5}}\,a'_{22}\lambda^4 & \sqrt{\frac{2}{5}}\,a'_{23}\lambda^2 \\ \frac{8}{5}\,a_{31}\lambda^6 & \sqrt{2}\,a_{32}\lambda^3 & r_b a_{33} \end{pmatrix}$$

$$Y_e(M_{GUT}) = \begin{pmatrix} \frac{6}{5}\,a_{11}\lambda^6 & 0 & 0 \\ \frac{4}{\sqrt{5}}\,a_{21}\lambda^5 & -3\sqrt{\frac{2}{5}}\,a_{22}\lambda^3 + \frac{12}{5\sqrt{5}}\,a'_{22}\lambda^4 & -3\sqrt{\frac{2}{5}}\,a'_{23}\lambda^2 \\ \frac{6}{5}\,a_{31}\lambda^6 & \sqrt{2}\,a_{32}\lambda^3 & a_{33} \end{pmatrix}$$

$$Y_\nu(M_{GUT}) \;=\; \begin{pmatrix} \sqrt{2}\,a''_{11}\lambda^8 & 2\,a_{12}\lambda^4 & 0 \\ 0 & \dfrac{6}{5\sqrt{5}}\,a'_{22}\lambda^4 & 2\,a_{23}\lambda \\ 0 & \dfrac{6}{5}\,a'_{32}\lambda^4 & r_\nu a_{33} \end{pmatrix}$$

where $\lambda = 0.22$ is the Wolfenstein parameter, and a and r are order unity coefficients which are precisely determined in the global fit to give excellent agreement with the observed quark and lepton masses and mixing angles. The numerical Clebsch factors are shown explicitly. Yukawa unification is not exact, with r_b for example dropping down to 0.7 for the best fits, although we keep $\tan\beta = 50$ fixed in our analysis.

The essential features of the flavour theory clearly include a large off-diagonal neutrino Yukawa coupling $Y^\nu_{23} \sim 1$, to generate the large atmospheric mixing angle, however in the quark sector the Yukawa matrices have small off-diagonal entries, and are not required to be symmetric. The flavour structure of this model is therefore typical of many $SO(10)$ models, and has no particularly unusual features, although of course we cannot claim it is generic since each $SO(10)$-like model will differ in the details of its flavour structure.

4 Results

We first summarise the experimental limits for the processes of interest:

$$\mathrm{Br}(B_s \to \mu\mu) \;<\; 2.0 \times 10^{-6}\,[\mathrm{CDF}] \tag{9}$$

$$\mathrm{Br}(B_d \to \mu\mu) \;<\; 6.1 \times 10^{-7}\,[\mathrm{Babar}] \tag{10}$$

with no bounds yet established for the τ final state processes. Looking to the future, the Tevatron will bring us further results for B_s decays with the prospect of a CDF bound in the region of $\mathrm{Br}(B_s \to \mu\mu) < 10^{-7}$. By comparison the standard model predicts $\mathrm{Br}(B_s \to \mu\mu)_{\mathrm{SM}} \sim 3.5 \times 10^{-9}$ [6].

To obtain predictions for such processes, we have performed a *top-down* global analysis of the $SO(10)$-like model outlined in the previous section. The analysis

[2] yields two distinct best fits, which we call Minimum A and Minimum B. The higgs spectrum in Minimum B is heavy, mostly above the TeV scale and will not be considered in the discussion below. The Higgs spectrum of Minimum A was found to be more interesting for our present study with masses at the 100 GeV scale. Hence it is the results from the unaltered fits of Minimum A which we present in this letter.

The numerical results for the processes $B_s \to \mu^+\mu^-$ and $B_s \to \tau^+\tau^-$ are displayed in fig. 1. Similar results for $B_d \to \mu^+\mu^-, \tau^+\tau^-$ are given in fig. 2. These results are presented as contour plots in the $m_F - M_{1/2}$ plane with a fixed value of $\mu = 120$ GeV(left panels) and $\mu = 300$ GeV(right panels). When comparing these contours with eq. 6 we find that a significant suppression is obtained from the ratio $\delta m_{d\,32}/m_b V_{ts}$. This comes purely from fitting the b quark mass, V_{cb} and $b \to s\gamma$.

The upper two panels of fig. 1 display contours of $\mathrm{Br}(B_s \to \mu\mu)$ with $\mu = 120$ and 300 GeV, and show values quite close to the current limits, and well above the standard model predictions. The Higgs mediated contribution in the SUSY model clearly dominates over the standard model contribution and for $\mu = 300$ GeV, with low $M_{1/2}$, it can even exceed the present CDF limit. An improved limit of 10^{-7} would be very restricting and could probe Higgs masses into the range, $m_{A^0} = 150{-}300$ GeV. As for the process, $B_d \to \mu\mu$, fig. 2 shows that the present bound is satisfied by both μ values over the entire displayed plane.

Inspection of figs. 1 and 2, reveals that the branching ratios for $B_{s,d} \to \mu^+\mu^-, \tau^+\tau^-$ are sensitive to the universal gaugino mass $M_{1/2}$, but not to the universal sfermion mass m_F. Inspecting the m_{A^0} panels of fig. 3 we see that it has a very similar $M_{1/2}$, m_F dependence. This is exactly as expected with a lighter mediating Higgs leading to larger branching ratios.

The branching ratio for $B_{s,\,d} \to \tau\tau$ is enhanced by a factor of $(y_\tau/y_\mu)^2 \sim 100$ compared to the muon final state processes, as can be seen in the lower panels of

fig. 1 and 2. This makes the tau final state processes very attractive for experimental discovery. The difficulty comes with the required detector resolution to measure tau decays. If this problem could be solved at future experiments then these tau final state processes could become the primary signal for indirect SUSY searches.

Fig. 3 contains corresponding contours of m_{A^0} in the upper panels and the quantity $\sin(\beta-\alpha)$, which controls the coupling of the lightest CP-even Higgs scalar coupling to the Z, in the lower panels. The numerical predictions for the best fit point at $M_{1/2} = 450$, $m_F = 500$ GeV (indicated by an asterisk in the figures) are given in Table 1.

	$\mu = 120$ GeV	$\mu = 300$ GeV
$M_{1/2}$ [GeV]	450	450
m_F [GeV]	500	500
$B_s \to \mu\mu$	1.5×10^{-6}	5.9×10^{-6}
$B_s \to \tau\tau$	2.6×10^{-4}	1×10^{-3}
$B_d \to \mu\mu$	1.5×10^{-7}	5.8×10^{-7}
$B_d \to \tau\tau$	2.7×10^{-5}	1×10^{-4}
m_{A^0} [GeV]	102	102
$\sin(\beta-\alpha)$	0.22	0.15

Table 1: Table of branching ratios for $B_{s,d} \to \mu^+\mu^-, \tau^+\tau^-$, CP-odd pseudoscalar mass m_{A^0}, and $\sin(\beta-\alpha)$ which governs the lightest CP-even scalar coupling to the Z, for the best fit point.

We now turn to the implications of a possible measurement (or an improved experimental limit) of the branching fraction of $B_s \to \mu\mu$ for $SO(10)$-like models. Fig. 4 and 5 show the effect on various quantities of varying the branching ratio for $B_s \to \mu\mu$ for three fixed points in the $m_F - M_{1/2}$ plane.

The upper panels of fig. 4 show the variation of χ^2 as $\mathrm{Br}(B_s \to \mu\mu)$ is varied. As $\mathrm{Br}(B_s \to \mu\mu)$ decreases the χ^2 increases initially slowly and later rapidly. The initial slow increase is understood from [2] where it was observed that the value of χ^2 for the best fit points are insensitive to changes of a few GeV in the Higgs spectrum,

which implies an insensitivity to small changes in the branching ratio for $B_s \to \mu\mu$. Hence the points which presently exceed the CDF bound can be forced to satisfy it with only a small(~ 0.5) increase in χ^2. But if the bound was to be lowered to 10^{-7} then this would no longer be possible with $\Delta\chi^2 \sim 3$. Hence the low $M_{1/2}$ region of the $\mu = 300$ GeV plane will be ruled out and the best fit region would move towards larger $M_{1/2}$.

The lower panels of fig. 4 display the variation of m_{A^0} as $\mathrm{Br}(B_s \to \mu\mu)$ is varied. As expected m_{A^0} increases smoothly as $\mathrm{Br}(B_s \to \mu\mu)$ decreases. Note the strong correlation of the CP-odd Higgs mass with $\mathrm{Br}(B_s \to \mu\mu)$, which for a fixed value of μ is quite insensitive to m_F and $M_{1/2}$.

The main contribution to the increase in χ^2 seen in fig. 4 is due to $b \to s\gamma$ not being fit well. The lower panels of fig. 5 show the variation of $\mathrm{Br}(b \to s\gamma)$ against $\mathrm{Br}(B_s \to \mu\mu)$ and show a clear correlation. This correlation was to be expected as the SUSY contribution to each of these processes involves the 23 mixings in the squark mass matrix. These panels also show why $b \to s\gamma$ is the main contribution to the change in χ^2 as the fit to $b \to s\gamma$ changes from within 1σ to almost 2σ.

The upper panels of fig. 5 show the variation of $\sin(\beta - \alpha)$ as $\mathrm{Br}(B_s \to \mu\mu)$ is varied. In the low $M_{1/2}$ region, where $\mathrm{Br}(B_s \to \mu\mu)$ is near the current limit, $\sin(\beta-\alpha)$ is small and hence the Z-boson couples predominantly to the heavier CP-even Higgs H^0, rather than the lighter Higgs h^0. However $\sin(\beta - \alpha)$ very quickly approaches unity as the $\mathrm{Br}(B_s \to \mu\mu)$ decreases, corresponding to the standard model limit where the h^0 couples like the standard model Higgs boson.

5 Conclusions

We have examined the potentially very promising signal $B_s \to \mu^+\mu^-$ in supersymmetry with large $\tan\beta \sim 50$ in a *top-down* approach starting from the best fits of an

$SO(10)$-like model studied recently. Our results go beyond minimal flavour violation investigated in previous works. Our results show that the absolute best fits provide for the $B_s \to \mu^+\mu^-$ signal at the borderline of the present limits and hence the ongoing search at the Tevatron will start having an impact on the global analysis of this class of SUSY models.

We have discussed the implications of a measurement (or an improved limit) of $B_s \to \mu^+\mu^-$ for restricting the parameter space of gauginos and sfermion masses, and of signals in other channels $B_{d,s} \to \ell^+\ell^-$. We have also discussed correlations of $B_s \to \mu^+\mu^-$ with $b \to s\gamma$ and the CP-odd Higgs mass. An improved limit for $\mathrm{Br}(B_s \to \mu\mu)$ of around 10^{-7} would be very restricting and could probe Higgs masses into the range, $m_{A^0} = 150 - 300$ GeV, with the Higgs coupling strength $\sin(\beta - \alpha)$ varying very quickly around this region. The possible non-observation of $B_s \to \mu^+\mu^-$ at the levels suggested by our study would by no means rule out $SO(10)$-like models. In the context of the analysis in [2] this would simply highlight Minimum B, with its heavier Higgs spectrum and $\mathrm{Br}(B_s \to \mu\mu) \sim 10^{-10}$, as the favoured solution. On the other hand we have seen that an actual observation of $B_s \to \mu^+\mu^-$ at the 10^{-7} level is quite plausibly expected in SUSY $SO(10)$-like models, with interesting phenomenological and theoretical consequences.

References

[1] K. S. Babu and C. F. Kolda, Phys. Rev. Lett. **84**, 228 (2000) [arXiv:hep-ph/9909476]. C. S. Huang, W. Liao, Q. S. Yan and S. H. Zhu, Phys. Rev. D **63**, 114021 (2001) [Erratum-ibid. D **64**, 059902 (2001)] [arXiv:hep-ph/0006250]. P. H. Chankowski and L. Slawianowska, Phys. Rev. D **63**, 054012 (2001) [arXiv:hep-ph/0008046]. C. Bobeth, T. Ewerth, F. Kruger and J. Urban, Phys. Rev. D **64**, 074014 (2001) [arXiv:hep-ph/0104284]. A. Dedes, H. K. Dreiner and

U. Nierste, Phys. Rev. Lett. **87**, 251804 (2001) [arXiv:hep-ph/0108037]. G. Isidori and A. Retico, JHEP **0111**, 001 (2001) [arXiv:hep-ph/0110121]. R. Arnowitt, B. Dutta, T. Kamon and M. Tanaka, Phys. Lett. B **538**, 121 (2002) [arXiv:hep-ph/0203069]. C. Bobeth, T. Ewerth, F. Kruger and J. Urban, Phys. Rev. D **66**, 074021 (2002) [arXiv:hep-ph/0204225]. A. Dedes, H. K. Dreiner, U. Nierste and P. Richardson, arXiv:hep-ph/0207026. A. J. Buras, P. H. Chankowski, J. Rosiek and L. Slawianowska, Phys. Lett. B **546**, 96 (2002) [arXiv:hep-ph/0207241]. J. K. Mizukoshi, X. Tata and Y. Wang, Phys. Rev. D **66**, 115003 (2002) [arXiv:hep-ph/0208078]. S. Baek, P. Ko and W. Y. Song, JHEP **0303**, 054 (2003) [arXiv:hep-ph/0208112]. G. Isidori and A. Retico, JHEP **0209**, 063 (2002) [arXiv:hep-ph/0208159]. A. J. Buras, P. H. Chankowski, J. Rosiek and L. Slawianowska, arXiv:hep-ph/0210145. C. S. Huang and X. H. Wu, Nucl. Phys. B **657**, 304 (2003) [arXiv:hep-ph/0212220]. T. Hurth, arXiv:hep-ph/0212304. T. Kamon [CDF Collaboration], arXiv:hep-ex/0301019. D. A. Demir, arXiv:hep-ph/0303249. A. Brignole and A. Rossi, arXiv:hep-ph/0304081. R. Dermisek, S. Raby, L. Roszkowski and R. Ruiz De Austri, JHEP **0304**, 037 (2003) [arXiv:hep-ph/0304101].

[2] T. Blazek, S. F. King and J. K. Parry, J. High Energy Phys. JHEP 05 (2003) 016, arXiv:hep-ph/0303192.

[3] R. Hempfling, Phys. Rev. D**49**, 6168 (1994). L. Hall, R. Ratazzi and U. Sarid, Phys. Rev. D**50**, 7048 (1994). M. Carena, M. Olechowski, S. Pokorski and C. Wagner, Nucl. Phys. B**426**, 269 (1994).

[4] T. Blazek, S. Raby and S. Pokorski, Phys. Rev. D **52**, 4151 (1995) [arXiv:hep-ph/9504364].

[5] C. Hamzaoui, M. Pospelov and M. Toharia, Phys. Rev. D **59**, 095005 (1999) [arXiv:hep-ph/9807350].

[6] A. J. Buras, arXiv:hep-ph/9806471.

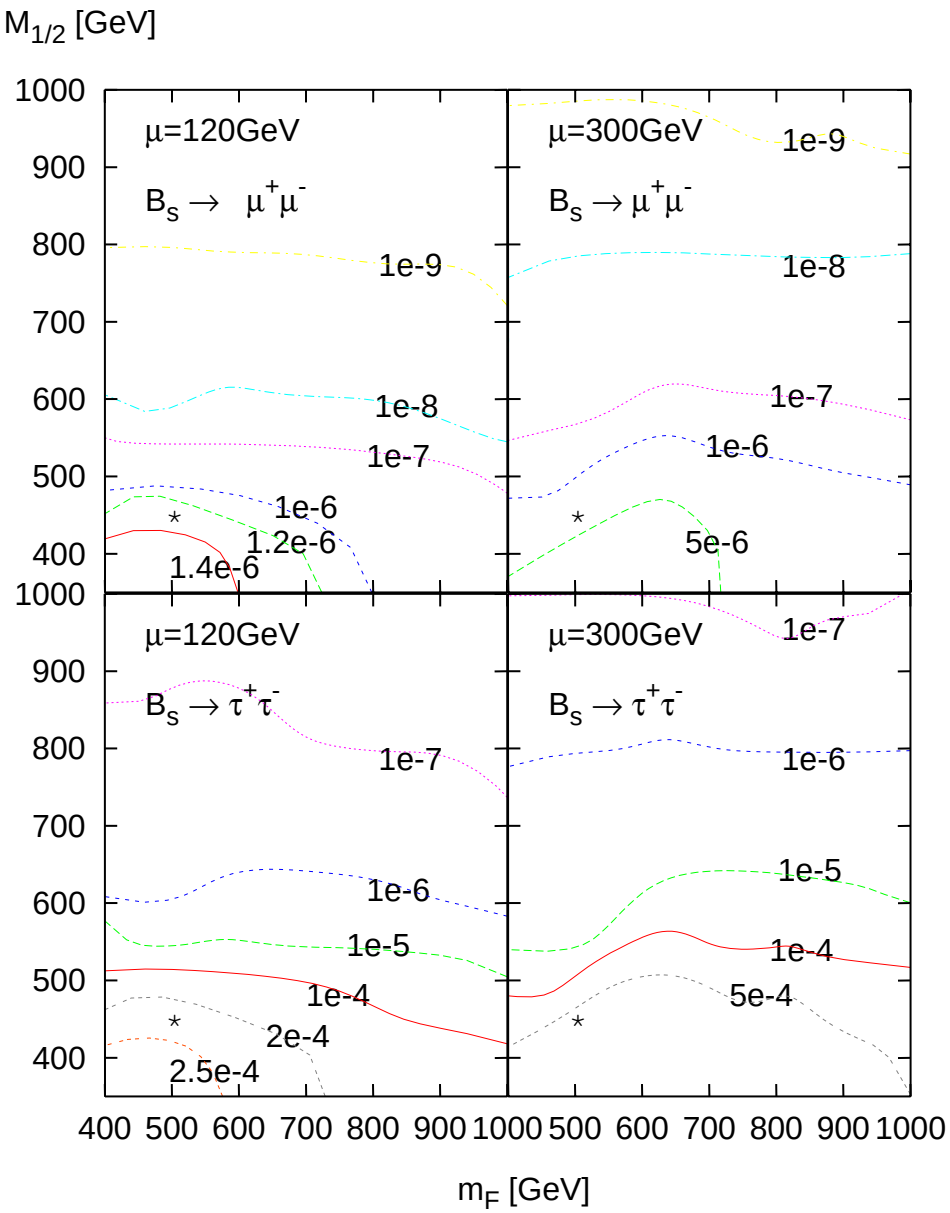

Figure 1: Contour plots for the branching ratios of the FCNC processes, $B_s \to \mu^+\mu^-$ and $B_s \to \tau^+\tau^-$. Each branching ratio is plotted with two different values of the μ parameter. The $\star$ marks the best fit point.

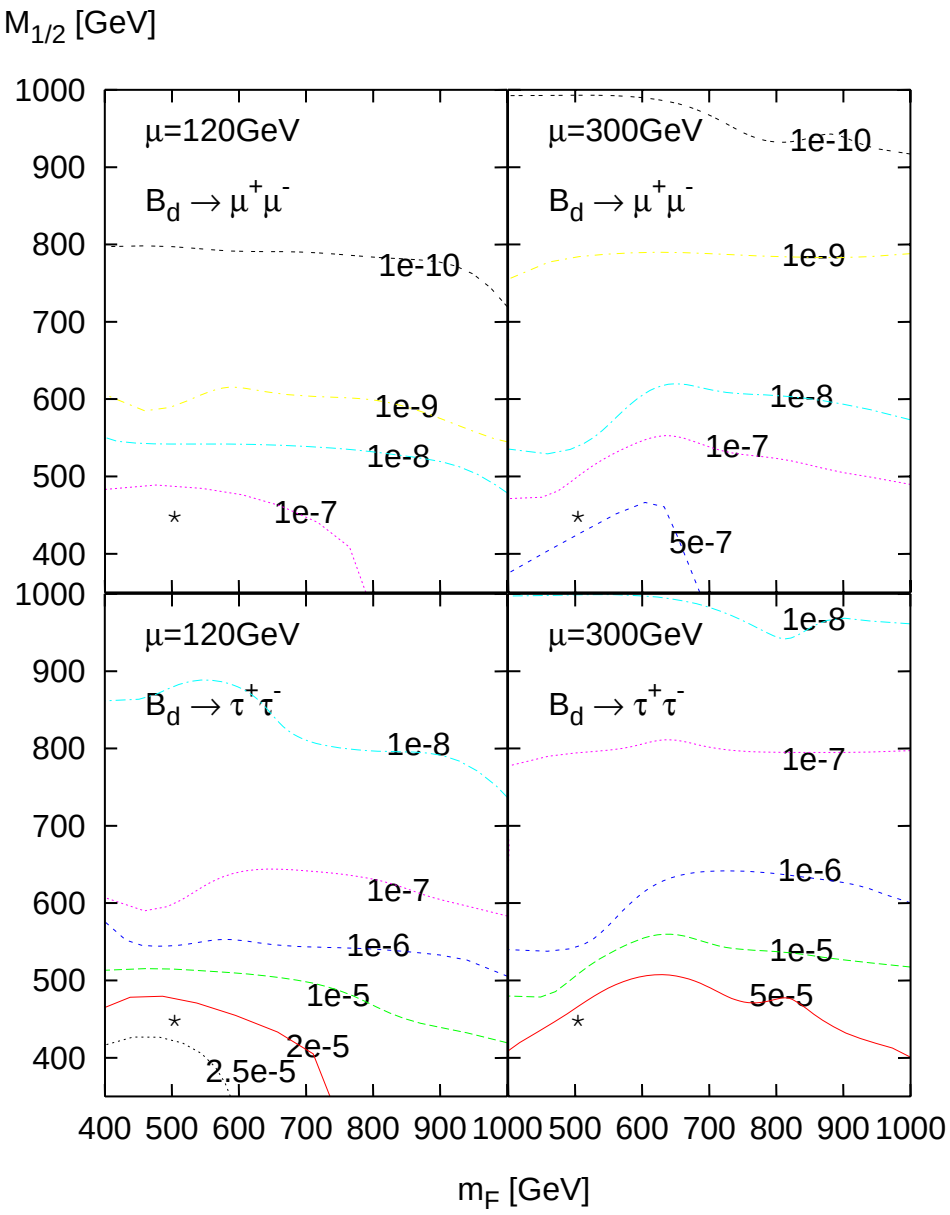

Figure 2: Contour plots for the branching ratios of the FCNC processes, $B_d \to \mu^+\mu^-$ and $B_d \to \tau^+\tau^-$. Each branching ratio is plotted with two different values of the μ parameter. The $\star$ marks the best fit point.

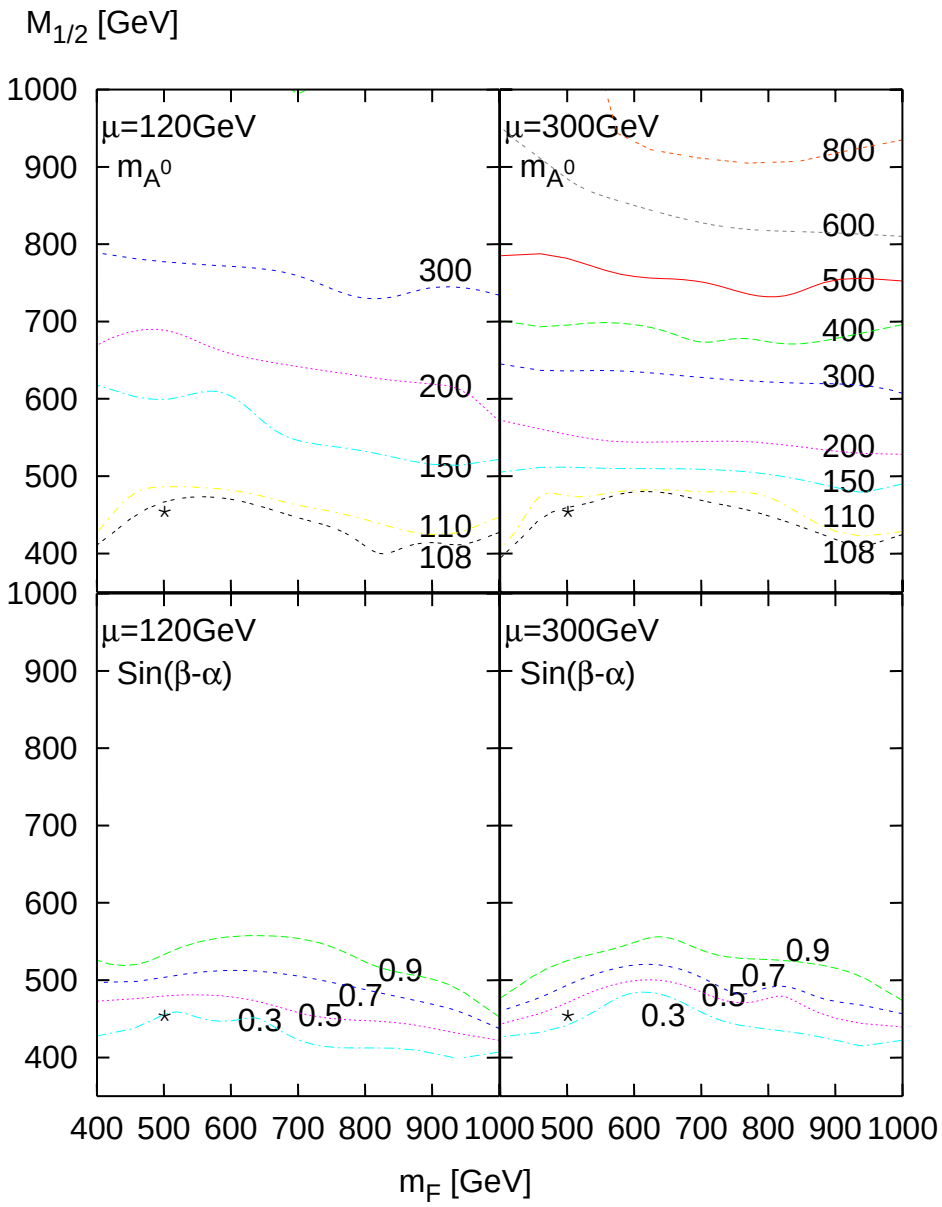

Figure 3: The upper two panels contain contours of the CP odd Pseudoscalar Higgs mass, plotted in the $m_F - M_{1/2}$ plane. The lower panels contain contours of, $\sin(\beta - \alpha)$, which determines the strength of the Z-boson coupling to, h^0, the lighter CP even Higgs. Again the plots are displayed at different values of μ. The $\star$ marks the best fit point.

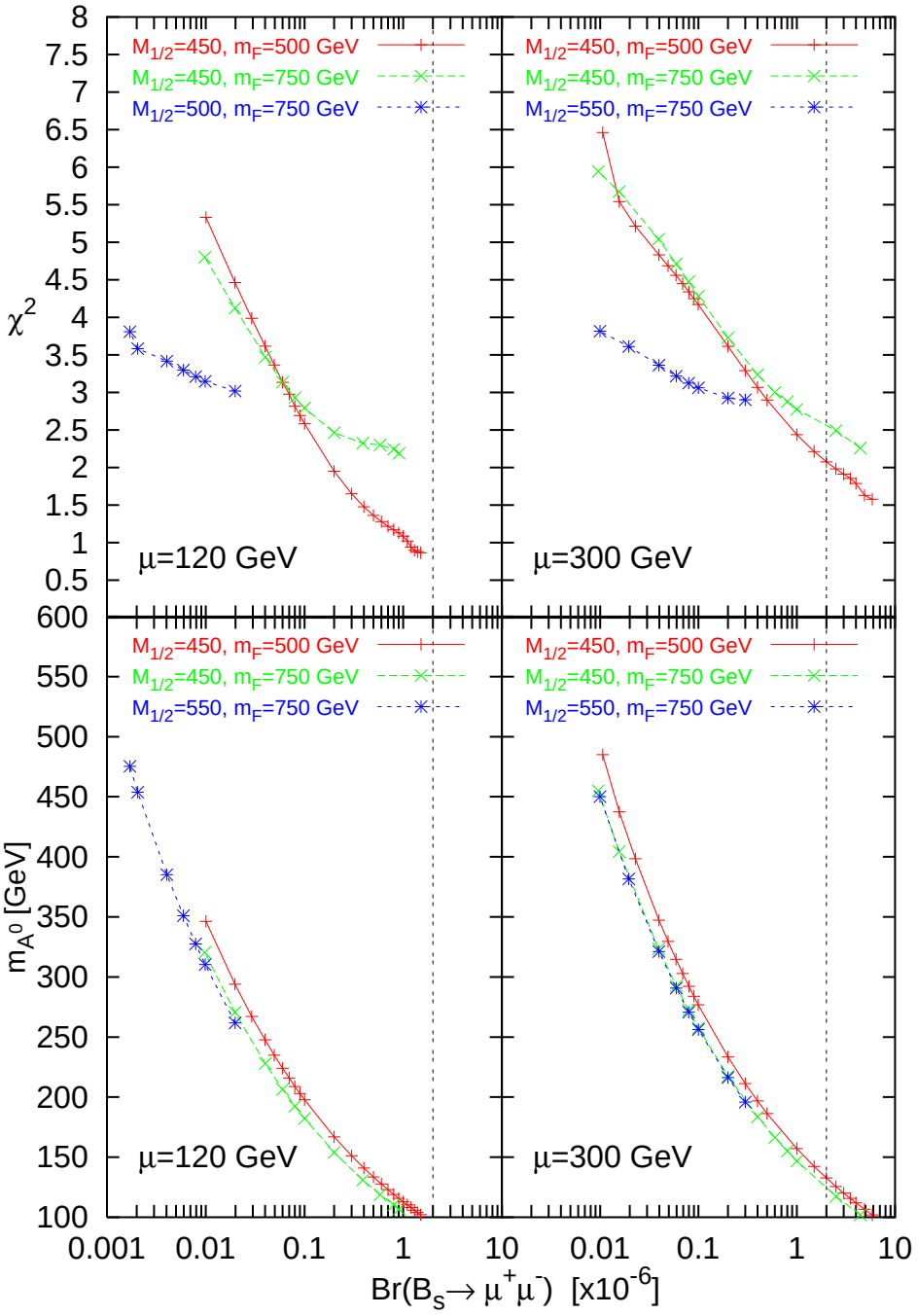

Figure 4: This figure shows the variation of χ^2 and the Pseudoscalar Higgs mass, m_{A^0}, as the branching ratio of $B_s \to \mu\mu$ varies from 10^{-5} down to 10^{-8}. Each of the three curves are drawn with fixed values of $M_{1/2}$, m_F. The vertical dashed line represents the present CDF bound on $B_s \to \mu^+\mu^-$.

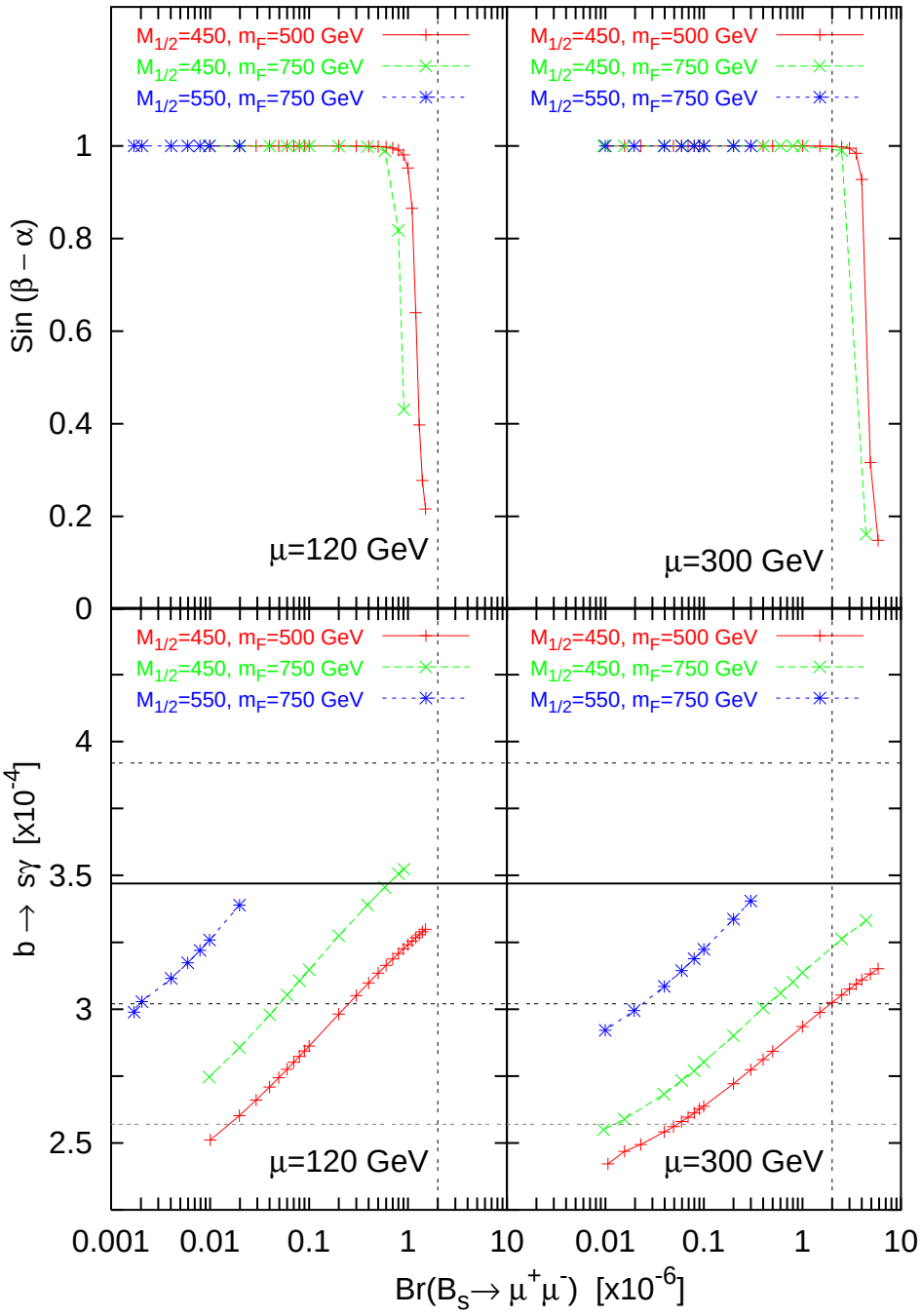

Figure 5: This figure shows the variation of $\sin(\beta - \alpha)$ and the branching ratio for $b \to s\gamma$, against $B_s \to \mu\mu$. The vertical dashed line represents the present CDF bound on $B_s \to \mu^+\mu^-$. The horizontal lines show the central measured value(solid) of $\mathrm{Br}(b \to s\gamma)$ along with the 1σ(dashed) and 2σ(light dashed) regions.